

Optical absorption, photoconductivity, and photoluminescence of glow-discharge amorphous $\text{Si}_{1-x}\text{Ge}_x$ alloys

B. von Roedern, D. K. Paul,* J. Blake,[†] R. W. Collins, G. Moddel,[‡] and William Paul

Division of Applied Sciences, Harvard University, Cambridge, Massachusetts 02138

(Received 4 December 1981; revised manuscript received 8 March 1982)

Results on the optical absorption, photoluminescence, and photoconductivity spectra and on electrical-transport data of amorphous $\text{Si}_{1-x}\text{Ge}_x\text{:H}$ alloys prepared from the plasma decomposition of silane and germane are presented. An attempt is made to find a self-consistent interpretation of the data in terms of changes in the optical energy gap and in the gap-state densities with mixtures of different ratios of SiH_4 to GeH_4 . It is found that the photoconductivity and the photoluminescence intensity are much higher than would be expected from the previously deduced values of the ratio of Si-H to Ge-H bonds from infrared absorption spectra. The principal conclusion of our results is that the changes in the intrinsic properties of a random tetrahedrally coordinated alloy as a function of alloy composition x are often masked by the extrinsic effects of changes with x in H content, defect density, and microstructure; the latter changes depend sensitively on the preparation method.

I. INTRODUCTION

Studies of semiconducting hydrogenated amorphous binary alloys are of particular interest because it is generally believed that, through an adjustment of the alloy composition, the optical and electronic properties can be tailored for device applications. We have reported earlier an important difficulty that may be encountered with hydrogenated binaries: Hydrogen may be found to be bonded preferentially to one of the elements, which may imply that defects associated with the less hydrogenated element are left in high density.¹⁻³ In this paper we shall discuss the electronic and optical properties of $a\text{-Si}_{1-x}\text{Ge}_x\text{:H}$ as a function of x , and thus examine the extent to which alloying and the concomitant changes in the H content and bonding result in a different density-of-states distribution than is observed in $a\text{-Si:H}$.

To aid the interpretation of the results, we invoke correlations between properties which have been established by more extensive studies on $a\text{-Si:H}$. Because the H content (c_H) and x are not independent parameters, ambiguities remain in distinguishing the effects of their variation on sample properties. To resolve these ambiguities it will be necessary to separate intrinsic effects (based on changes in the properties of the random, completely tetrahedrally coordinated, homogeneous alloy) from the extrinsic effects of changed c_H , H-bonding configurations, defect density, and microstructure.

In concurrent work on the $a\text{-Si}_{1-x}\text{Ge}_x\text{:H}$ system, Hauschildt *et al.*⁴ have interpreted their results in terms of an increase in the defect state density in the gap and a decrease in the extent of the band tails with increasing x . For our samples we deduce similar changes with x in the midgap density of states, but we find an increase or a decrease in the extent of the conduction-band tail, depending on the deposition technique. We infer that there are both intrinsic and extrinsic contributions to the density of states in the conduction-band tail for our samples.

II. SAMPLE PREPARATION

All samples were deposited on the cathode of a dc glow-discharge apparatus built from glass and

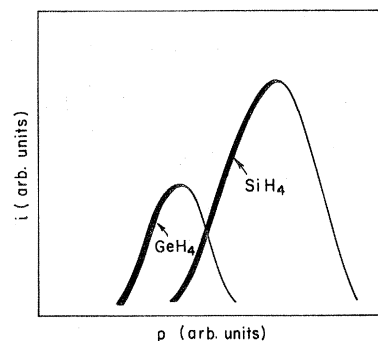


FIG. 1. Schematic discharge characteristic of the dc glow-discharge plasma of SiH_4 and GeH_4 . Samples were deposited in the low-pressure regimes indicated by the heavy lines.

TABLE I. Characteristics of the α -Si_{1-x}Ge_x:H alloys of this study.

Sample	Substrate temperature (°C)	Film thickness (μm)	Rate of deposition (μm/min)	Ge content microprobe 100×	Composition	
					H content (at. %) Evolution	ir absorption wag mode
Ge GD1	250	6.5	0.54	100		2.6
Ge GD2	250	14	0.40	100	8.6	2.6
Ge GD4	100	5.0	0.13	100	10	5.0
SiGe GD1	250	9.3	0.46	90		3.2
SiGe GD4	250	3.9	0.26	88		3.9
SiGe GD9	250	12	0.22	82	18	9.4
SiGe GD12	100	6.0	0.20	70	38	23
SiGe GD8	250	12	0.20	68	10	9.1
SiGe GD14	250	6.6	0.19	65	13	9.5
SiGe GD3	250	5.0	0.25	55		8.0
SiGe GD2	250	5.5	0.28	42		11
SiGe GD6	250	3.5	0.14	28		10
SiGe GD7	250	3.6	0.14	26		12
SiGe GD13	250	8.0	0.14	14	15	9.2
Si GD4	250	11	0.16	0	8	11
Si GD10	100	11	0.18	0	15	12

stainless-steel components. The pumping system consisted of a liquid-N₂ cold trap, a diffusion pump and a roughing pump. The adjustable electrode gap was set at 13 mm, and the diameter of anode and cathode electrodes was 37 mm. The dc plasma was excited with 900 V, and the SiH₄ and GeH₄ pressures were adjusted such that the current was maintained between 0.8 and 2.0 mA. The discharge characteristic of the dc plasma was found to be critical to the properties of the films. Figure 1 shows a qualitative relationship between the discharge current i at a fixed voltage as a function of the pressure p of pure silane or germane. All our samples have been prepared under low-pressure conditions (heavily lined part in Fig. 1). Since i varies rapidly with p , the discharge current is a sensitive indicator of the pressure and was monitored to aid in the adjustment of p . This procedure avoided the deposition of "polysilane"-type α -Si:H samples, which have been reported to nucleate from high-pressure SiH₄ plasmas.⁵

Films were codeposited on glass (Corning 7059), crystalline Si, and aluminum substrates, at substrate temperatures of 100 and 250°C. The rate of deposition on the conducting substrates, which was about 5 times faster than on the glass substrates, varied between 0.1 and 0.5 μm/min as x was increased from 0 to 1. Table I summarizes the characteristics of the samples. The thicknesses and deposition rates shown there are for samples on

crystalline Si substrates. The thicknesses for these samples were determined to an accuracy of ~10% by an edge-on scanning electron microscopy measurement.

III. CHEMICAL AND STRUCTURAL CHARACTERIZATION

The amorphicity of the films was verified by x-ray diffraction, and their composition determined by electron microprobe, with an overall accuracy of ±1%. The microprobe used a wavelength dispersive spectrometer and was interfaced with a microcomputer that compared the intensities of Si and Ge with crystalline standards and corrected for background and matrix effects. Probes of the composition at several spots of the sample surface indicated uniformity within the sensitivity of the experiment (1 μm spot size).

A study of the films by secondary ion mass spectroscopy (SIMS) (performed by Charles Evans Associates) provided information on the depth profile of various constituents. In principle, it is also possible to obtain the concentrations of the constituents by SIMS, but the sensitivity factors of different elements depend strongly on the atomic matrix of the sample. As a result, an absolute quantitative estimation may be in error by as much as a factor of 2. Figure 2 shows a typical depth profile

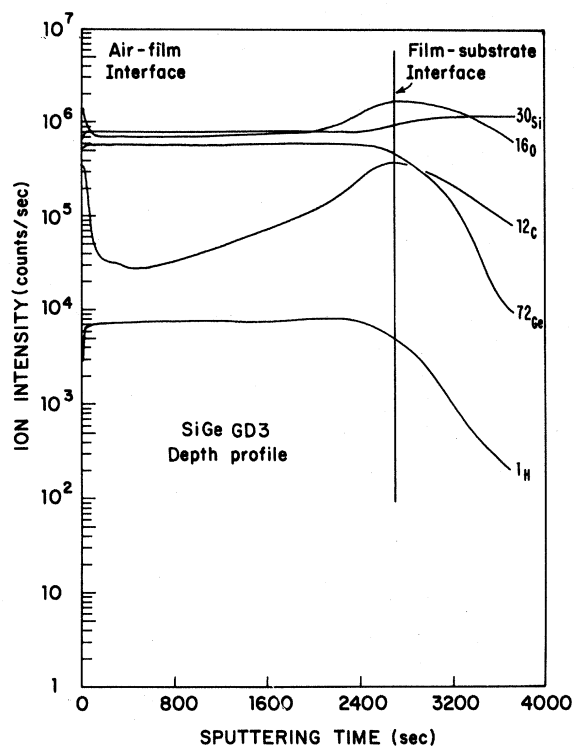


FIG. 2. SIMS depth profile of constituents of film SiGe GD3.

of various elements. The most important result of the SIMS study is the establishment of the uniformity of the Si and Ge content throughout the film thickness. Occasionally, a build-up of contaminants such as O and C was observed within 500 Å of the interface between the film and the substrate. The bulk levels of O and C are estimated to be $\sim 10^{20}$ and $\sim 5 \times 10^{19} \text{ cm}^{-3}$, respectively. The following facts suggest that it is unlikely that the properties reported here are influenced by the observed contaminant levels. We recall that the electronic and optical properties of our sputtered α -Si:H do not seem to be altered by C or O contents of similar magnitude. Changes in these properties *do* occur at deliberately introduced higher O concentrations, when clear signatures of Si-O entities appear in the infrared vibrational absorption spectra of 1- μm thick films.⁶ However, no such absorption is discerned in films of the alloy series reported here, even in the 12- μm thick samples.

The H content c_H of the samples as measured by evolution or by the integrated absorption of the infrared wag modes at $\sim 600 \text{ cm}^{-1}$ is given in Table I. In Fig. 3, c_H is plotted as a function of the composition x for the samples prepared at a substrate temperature of 250°C. The difference between the c_H values obtained from infrared and

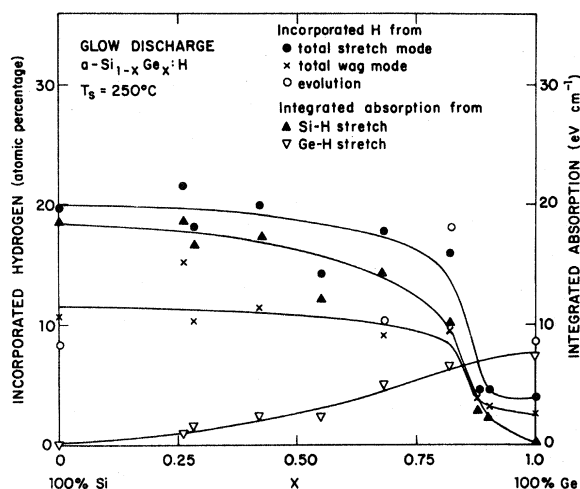


FIG. 3. Hydrogen content c_H of the samples as a function of composition x . Details concerning the determination of c_H may be found in Ref. 3.

evolution has been attributed to weakly bonded hydrogen in the Ge-rich samples.³ The weakly bonded hydrogen which evolves at low temperatures has a different effect on the electronic and optical properties than that bonded in SiH or SiH₂ configurations.⁷ When it is evolved, the photoluminescence intensity does not change significantly, although there is a small shift of the peak to lower energies attributable to a network relaxation effect. We conjecture that the principal effect of the weakly bonded hydrogen is a perturbation in the structure of the network. Transmission electron microscope pictures of the Si-rich samples did not reveal microstructure, whereas a pure glow-discharge α -Ge:H film prepared at a substrate temperature of 100°C showed density fluctuations on a scale of 100 Å.⁸

IV. RESULTS

A. Optical absorption

The optical absorption edges $\alpha(h\nu)$ were measured using a Cary 14 double beam spectrometer. For samples on glass substrates, we obtained an average value of the film thickness either from a direct measurement with a Sloan Dektak at several points of the film surface, or from an analysis of the interference fringes using a thin-film optical program. We conclude that, despite inhomogeneities in film thickness, α may be determined with sufficient accuracy to give E_{04} (the energy for which α equals 10^4 cm^{-1}) within $\pm 0.03 \text{ eV}$.

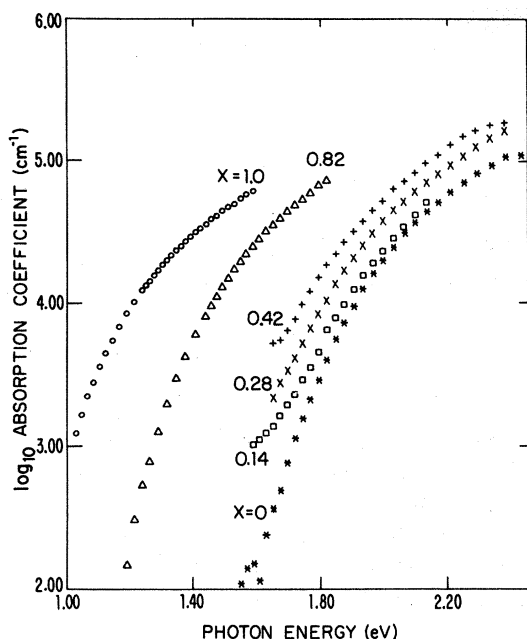


FIG. 4. Absorption edge spectra for representative alloys.

A selection of optical absorption spectra is shown in Fig. 4. Keeping in mind the variation of c_H with x of Fig. 3, we observe that the position of the absorption edge is affected by the alloy composition. Figure 5 shows the variation of the optical parameters with composition x . We have plotted E_{04} and E_g , where the latter is found by extrapolation of $(ah\nu)^{1/2}$ vs $h\nu$ to $\alpha=0$. We must point out that the extrapolated value E_g depends on the region of α from which the extrapolation is made, because the $(ah\nu)^{1/2}$ vs $h\nu$ curve is not exactly a

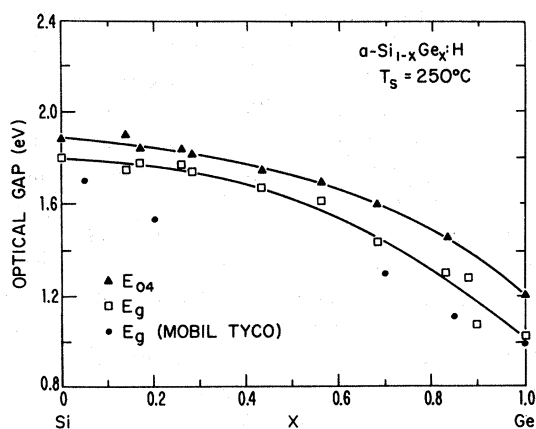


FIG. 5. Variation of the optical parameters E_{04} and E_g with x . This figure also includes some data points (labeled Mobil Tyco) for samples produced by rf glow discharge by Cretella (Ref. 22).

TABLE II. Values of ΔG and E_σ for $a\text{-Si}_{1-x}\text{Ge}_x\text{:H}$ alloys.

Sample number	x	E_σ (eV)	ΔG ($\Omega\text{ cm}$) ⁻¹
Si GD1	0	0.93	7.2×10^{-7}
SiGe GD7	0.26	0.74	1.9×10^{-7}
SiGe GD6	0.28	0.86	2.3×10^{-9}
SiGe GD2	0.42	0.85	5.1×10^{-8}
SiGe GD3	0.55	0.85	8.8×10^{-10}
SiGe GD8	0.68	0.82	2.4×10^{-10}
SiGe GD9	0.82	0.74	1.5×10^{-10}
SiGe GD4	0.88	0.67	1.6×10^{-9}
Ge GD1	1.00	0.46	3.1×10^{-9}

straight line. We have chosen to perform the extrapolation from the region of high α ($\sim 10^4$ to $\sim 10^5\text{ cm}^{-1}$), and as a result obtain larger values of E_g than Onton *et al.*⁹ For the Ge-rich alloys, these authors have performed the extrapolation from data at significantly lower α . For these samples we believe α might be influenced by gap state absorption.

B. Photoconductivity

A full description of the apparatus used has been reported elsewhere.¹⁰ The photoconductive re-

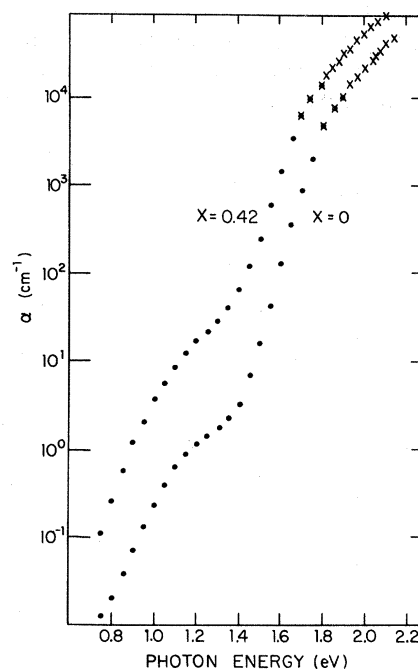


FIG. 6. Photoconductivity derived absorption spectra for samples Si GD1 and SiGe GD2 (circles). Crosses denote data obtained from a direct optical absorption measurement.

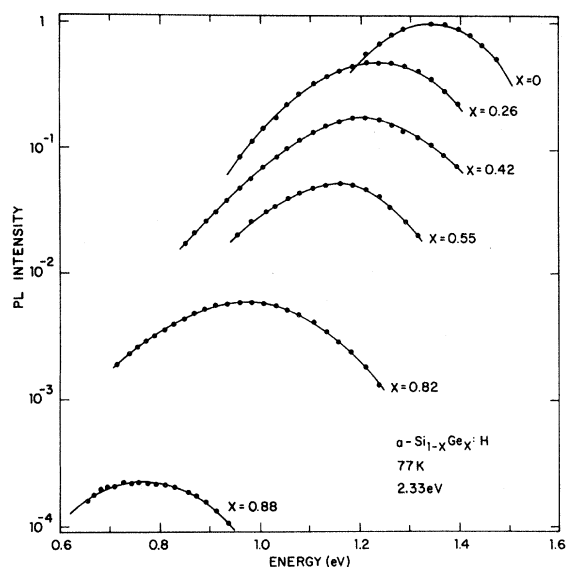


FIG. 7. Photoluminescence spectra for representative alloys.

sponse ΔG has been measured under “standard” conditions (1.96-eV excitation and 10^{15} photons/cm²). Although ΔG can scatter by as much as an order of magnitude for a given x , there is a clear decrease of about 3 orders of magnitude as x is increased from 0 to 0.6, and an increase by a factor of about 20 as x is further increased to 1.0 (see Table II).

From the spectral dependence of ΔG , the absorption coefficient has been derived for the energy range between 0.8 eV and the region where it can

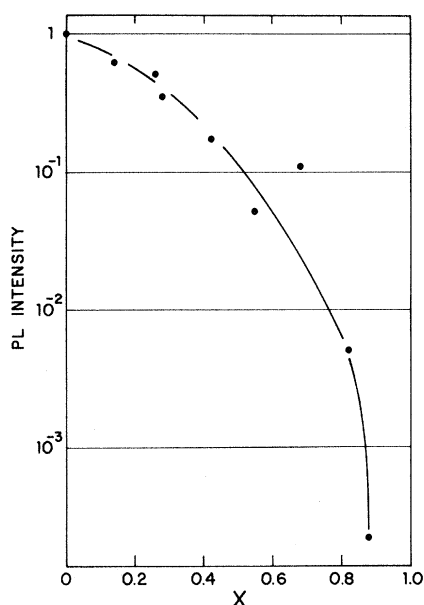


FIG. 8. Variation of the PL peak intensity with x .

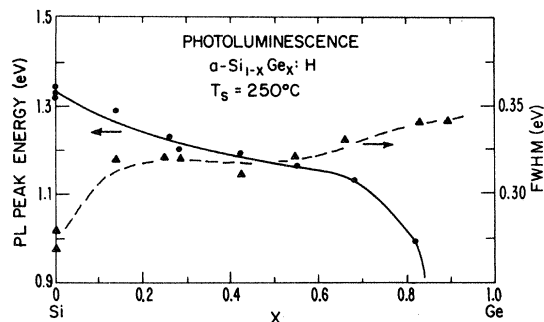


FIG. 9. Variation of the FWHM and peak energy of the PL with x .

be found from a direct absorption measurement.¹⁰ Figure 6 shows the extended absorption spectra for samples with $x=0$ and 0.42. We note that the $\alpha(h\nu)$ curves both show structure below an approximately exponential behavior near $\alpha=10^3$ cm⁻¹, analogously to what is found for pure a -Si:H.¹⁰

C. Photoluminescence

We have also characterized the alloys by parameters derived from the photoluminescence (PL) spectra. A description of the PL apparatus and data evaluation is given elsewhere.¹¹ Figure 7 shows the deconvoluted PL spectra of some representative samples. In Fig. 8 we show the dependence on x of the PL intensity and in Fig. 9 the dependences on x of the full width at half maximum (FWHM) and the peak position in energy. We observe a decrease in the PL intensity by nearly 4 orders of magnitude as x is increased to 0.9; no PL was detected for $x=1.0$. There is a single PL band at all compositions with a peak position that shifts to lower energy with increasing x , first gradually for $x < 0.6$, and then more steeply for $x > 0.6$. The PL FWHM is observed to increase with increasing x . When x is increased to 0.6, we also note a decrease in the slope of the log (PL intensity) with temperature. In glow-discharge films with $x=0$, measured at 150 K, a superlinearity has been observed in the luminescence intensity as a function of excitation intensity, and interpreted as evidence for a nongeminate component in the radiative recombination.¹² We have confirmed this effect for several of our glow-discharge samples with $x=0$. Only one of the samples for $x > 0$ (SiGe GD8 with $x=0.68$) was measured as a function of excitation intensity at different temperatures. No significant superlinearity was observed in the excitation intensity dependence of the PL for this sample for temperatures as high as 200 K.

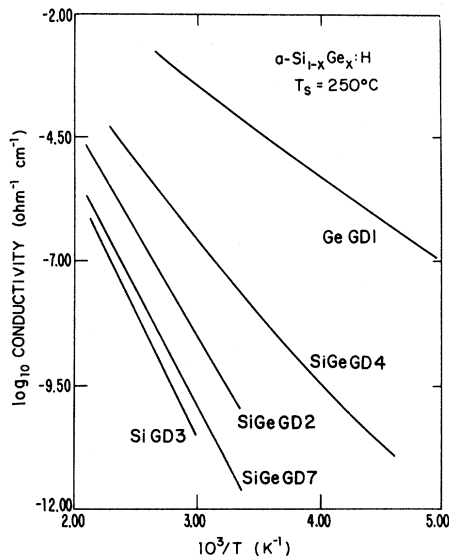


FIG. 10. Conductivity vs $10^3/T$ for samples of different x .

D. Electrical transport

The dc conductivity measurements were made using coplanar Nichrome contacts. The temperature dependence of the conductivity $\sigma(T)$ for several alloys is shown in Fig. 10. It is seen that there is a wide range in T of activated transport, adequate to define the parameters E_σ and σ_0 in the relation

$$\sigma(T) = \sigma_0 \exp[-(E_\sigma/kT)]. \quad (1)$$

Figure 11 displays the variation of the deduced parameters E_σ , σ_0 , and σ_{RT} (room-temperature conductivity) with composition x . A list of E_σ values is given in Table II. It is observed that with increasing Ge content, σ increases at all temperatures. E_σ remains relatively unchanged near 0.85 eV for $x < 0.6$, and then decreases rapidly to 0.5 eV as x approaches 1. The trend in σ_0 is less

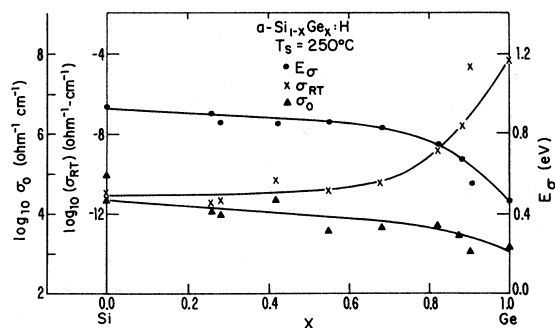


FIG. 11. Transport parameters σ_0 , σ_{RT} , and E_σ as a function of x .

dramatic. Despite considerable scatter in the values for σ_0 , the average value of σ_0 for a -Ge:H seems to be nearly an order of magnitude smaller than that for a -Si:H.

V. DISCUSSION

In attempting to interpret the band-structure and electronic processes in a -Si:H, a number of properties other than those reported here are studied. The results from them may be exploited to help to interpret the properties measured for the a -Si $_{1-x}$ Ge $_x$:H alloys, and derive information about the density of states near midgap and at the conduction- and valence-band edges.

The variation of the density of states (DOS) with energy just above the valence-band edge, determined from photoemission measurements, has been found to correlate with the variation in the absorption coefficient at subband gap energies in undoped and P-doped a -Si:H.¹³ This suggests that the increase of α near 1.2 eV in the shoulder of the $\alpha(h\nu)$ curve of Fig. 6—even taking into account the shift to lower energies of the intrinsic absorption edge—reflects an increase in the DOS above the valence-band edge. However, similar reasoning cannot be applied to the $\alpha(h\nu)$ data for larger x , where the intrinsic edge has shifted further.

The midgap density of states may be deduced from measurements of the capacitance and conductance as a function of frequency at zero bias in a -Si:H Schottky diodes.¹⁴ It has been shown¹⁵ that this midgap density of states correlates very well both with the magnitude of $\alpha(h\nu=1.2$ eV) and the inverse of the PL magnitude measured on codeposited a -Si:H samples. Thus, the well-established decrease in the PL magnitude over the entire range of x in Fig. 8, as well as the more limited analysis possible from the photoconductivity spectra, may be taken as a manifestation of an increase with x of the midgap state density.

The photoluminescence FWHM, the shape of the temperature dependence of the photoluminescence intensity,¹⁶ and the electron drift mobility activation energy¹⁷ are argued to provide information about the density of states below the conduction-band edge E_0 which is usually taken to vary as

$$N_c(E) = N_{c0} \exp[(E - E_0)/E_c]. \quad (2)$$

(1) *The photoluminescence FWHM.* This assumes that the sample-to-sample variations in the spread in recombining electron energies can be at-

TABLE III. Values of T_0 , obtained from the temperature dependence of the photoluminescence intensity [see Eq. (3)], FWHM, the full width at half maximum of the photoluminescence spectrum, and $E_{\mu d}$, the electron drift mobility activation energy for a -Si:H, a -Si $_{1-x}$ Ge $_x$:H, and related materials prepared by glow discharge (gd) and sputtering (sput). The totality of parameters for all of the alloys is not indicated here since the table is designed to show a correlation of FWHM, T_0 , and $E_{\mu d}$ with conduction-band-tail state density.

Material	Preparation technique	(Sample number)	T_0 (K) ± 1 K	FWHM (eV) (± 0.01)	$E_{\mu d}$ (eV)
a -Si:H	rf gd	(MT)	16	0.26	0.12
a -Si:H	dc gd	(5)	21	0.28	0.15
a -Si $_{0.43}$ Ge $_{0.57}$:H	sput/gd	(6#2)	25	0.29	
a -Si:H	sput	(100)	27	0.33	0.23
a -Si $_{0.32}$ Ge $_{0.68}$:H	dc gd	(8)	29	0.33	
a -Si:H	sput	(151)	31	0.35	
a -Si:H:F	dc gd	(3)	53	0.43	
a -Si:O	sput	(162#2)	68	0.64	

tributed in part to variations in the DOS below the conduction-band edge. The FWHM then gives a relative measure of E_c .

(2) *The parameter T_0 describing the decrease in PL intensity I with increasing temperature.* T_0 is defined by¹¹

$$[I(T \rightarrow 0)/I(T)] - 1 = \exp(T/T_0). \quad (3)$$

This supposes that nonradiative recombination proceeds via activation of the electron out of the exponential conduction-band tail,¹⁶ and it is the distribution of occupied states in the tail that determines T_0 . Thus T_0 is directly proportional to E_c .

(3) *The electron drift mobility activation energy $E_{\mu d}$ obtained from a combination of steady state photoconductivity measurements and the photoconductivity decay after excitation is removed.* This again supposes that electron activation out of an exponential tail of trapping states determines the rate of photoconductivity decay. $E_{\mu d}$ is then proportional to both T_0 and E_c .

Values of the FWHM, T_0 , and $E_{\mu d}$ for several different types of sample are shown in Table III; they correlate satisfactorily according to the above assumptions. Thus we can use any of the three parameters, FWHM, T_0 , and $E_{\mu d}$ as a relative measure of the conduction-band-tail state density. This demonstrates that the sample-to-sample variations in the PL FWHM reflect changes in the DOS distribution below E_c , rather than changes in the electron-phonon coupling. We shall employ this conclusion in interpreting the results for

a -Si $_{1-x}$ Ge $_x$:H, using the FWHM as the primary indicator of the tail state DOS below E_c .

The values of E_g and E_{04} are determined by two factors: (1) the distribution in energy of the conduction- and valence-band densities of states associated with the completely coordinated, although topologically disordered network. These states may be extended, or localized in the band tails. (2) The distribution in energy of localized states associated with defects (dangling bonds, etc.) in the disordered network and with impurities. Both factors are assumed to depend on x and c_H in a hydrogenated binary system, and it has been explicitly demonstrated¹⁸ that they depend on c_H for $x=0$. Thus, for any alloy composition, it is necessary to inquire whether x or c_H is the principal determinant of the optical gaps (note that, from Fig. 3, c_H changes rapidly for $x > 0.6$). An additional complication develops when one considers that for a given c_H and x , the H-bonding configurations will also influence both (1) and (2) above. This was shown explicitly in a comparison of glow-discharge and sputtered a -Si:H.¹⁷ From the trends in Fig. 5, showing a very small decrease in optical gap with increasing x for $x \leq 0.6$, it appears that the actual alloying of Si with Ge has little effect on E_{04} , i.e., on the distribution of valence- and conduction-band states. If a contribution to $\alpha(h\nu)$ data in Fig. 4 exists due to defect states nearer midgap which increase in density with increasing x (as deduced from the PL result in Fig. 8), this conclusion is further strengthened.

The decrease in the photoconductance of the al-

loy implies a decrease in the electron $\mu\tau$ product. It is to be noted, as an aside, that such a decrease is probably not the sole cause of poor device performance in the alloys. Poor solar cell performance is more directly related to a low $\mu\tau$ product for holes. Since we know that, in a -Si:H,^{6,15} this can be correlated with an increase in α (1.2 eV), it may be that the observed increase in the low-energy absorption coefficients for the alloy in Fig. 6 implies the poorer device performance actually found.

Table II shows that there is considerable scatter in the values of ΔG for similar values of x . Similar scatter is found when parameters are varied in the preparation of unalloyed a -Si:H, but when ΔG is plotted versus E_σ , a clear exponential relation is found.¹⁹ This dependence has been variously attributed to increased hole trapping as the Fermi level rises, which sensitizes the electron photoconductivity, and to a decrease in recombination center density as the Fermi level rises. Whatever the cause, the scatter of ΔG with x may be linked with fluctuations in E_σ , and these in turn attributed to the sensitivity of E_σ , or the Fermi level position, to variations in accidental doping or defect density. If we somewhat arbitrarily adjust the present ΔG data by dividing out the empirical dependence^{15,19} of ΔG on E_σ observed for sputtered and glow-discharge a -Si:H, then the increase in ΔG with x for $x > 0.7$ is eliminated and the scatter in the adjusted values is significantly less.

The increase in the PL FWHM with increasing x suggests, in light of the correlation in Table III, that the conduction-band (CB) tail increases in extent with x for these alloys. This is consistent with increased disorder, but these data alone are insufficient to determine its precise nature (whether fluctuations in bond length, bond angle, dihedral angle, or any other cause). It is pertinent to note immediately that this result is *not* a general one for such alloys. Hauschildt *et al.*⁴ report that, in contrast, the FWHM decreases linearly with increasing x for their alloys produced by glow discharge. Recently we have prepared a -Si_{1-x}Ge_x:H by sputtering a c -Si target in (H₂ + GeH₄ + Ar). For this material²⁰ also, both T_0 and the FWHM were somewhat smaller than observed for typical sputtered a -Si:H. (See third entry in Table III. For a discussion of the variation of the FWHM with x for a larger set of these samples, see Collins and Paul, Ref. 16.) It would seem reasonable that the CB tail of least extent among materials of the same alloy composition is closest to revealing the

intrinsic DOS (due to intrinsic topological disorder). From this viewpoint the broadening of the CB tail observed in our similar composition pure glow-discharge alloys must be attributed to some cause other than Si-Ge mixing; among speculative possibilities are H-induced defects and/or microstructural changes resulting from the particular combination of preparation parameters used here.

The decrease in the PL intensity and loss of nongeminate recombination with Ge incorporation suggests an increase in the density of nonradiative recombination centers which may capture conduction-band electrons directly and/or provide sites to which band tail electrons may tunnel. Simple dangling-bond defects may be the important nonradiative centers.¹² It is relevant, at this juncture, to point out that a preference ratio of 10 for Si-H over Ge-H bonds, and a total H content of 10 at. % in, say, an alloy with $x=0.5$, correspond to a Ge film hydrogenated only to $c_H=2$ at. %. A sputtered a -Si:H film of this c_H would have a PL peak intensity at least 2 orders of magnitude smaller than that actually observed for our $x=0.5$ alloy. We conclude that, despite the fact that the Ge-H configuration is much less likely than Si-H, there is *not* a correspondingly high density of nonradiative recombination centers (dangling bonds) associated with defects on the Ge. This is an important new conclusion which deviates from our earlier speculations on the consequences of preferential attachment of H. We suggested earlier³ that preferred Si-H bonding might result in a higher ESR signal arising from dangling bonds on the less hydrogenated element. The PL result does not support this. Morimoto *et al.*²¹ measured a single line ESR signal in a -Si_{1-x}Ge_x:H and, on deconvoluting it in terms of the lines observed in pure a -Si:H and pure a -Ge:H, inferred a dominant Ge-type resonance contribution, where the ratio between Ge dangling bonds and Ge atoms decreases drastically with increasing x . This is in agreement with our interpretation of the meaning of our PL results.

We shall next comment on the nonlinear variation with Ge content of the gap size given by E_{03} or E_{04} . Onton *et al.*,⁹ Hauschildt *et al.*,⁴ and Cretella²² have all found a linear variation of gap with x and a difference between the gaps (however defined) for $x=0$ and $x=1$ of about 0.6 eV. In these works no attempt was made to distinguish the effects of alloying or hydrogenation in determining the size of the gap; however, since the quoted gaps are, for all x , smaller than ours, we infer that the film H contents were smaller and the

gaps therefore less susceptible to variations in H content than for our films. It is notable, however, that the *total* gap change in our samples is also 0.6 eV. The more rapid decrease in gap with x between 0.6 and 1.0 is qualitatively consistent with the decrease in c_H with x shown in Fig. 3, but the relatively small variation in gap with x between 0 and 0.6, where c_H is almost constant, requires some new element of explanation. There is as yet insufficient evidence for a firm conclusion, but two general speculations may be made on circumstances which *could* lead to the observed result. The first is that the effects of alloying and hydrogenation on the conduction- and valence-band edge states, and thus on the energy gap, are not simply additive for all x and c_H . The second is that the distribution of H between compensated dangling bonds, weakly bonded entities, etc., may change with x while $c_H(\text{total})$ remains constant, and that the different distributions have different effects on the overall state density function. Whether these speculations are correct or not, it is essential that the point be made that, in assessments of the properties of hydrogenated binary alloys, consideration must be given not only to the alloying of the two elements but also to the hydrogen content, its bonding configuration, and the microstructure which may be a function of c_H and x .

VI. CONCLUSIONS

From this work we have drawn the following principal conclusion: The precise changes in the conduction- and valence-band densities of states, and in the pseudogap density of states, of $a\text{-Si}_{1-x}\text{Ge}_x\text{:H}$ alloys as a function of x , depend intimately on changes in both x and c_H , and through them on the details of the preparatory method. When the same apparatus and procedures were used to prepare the alloys by dc glow discharge from mixtures of decreasing ratios of SiH_4 to GeH_4 , the changes in the optical absorption, photoconductivity and photoluminescence spectra, and in electrical-transport data, could be self-consistently interpreted to infer a decreased optical gap and increased state densities in the band tails and near midgap. However, several factors prevent the deduction of changes in the *intrinsic* band structure of the random tetrahedral alloy distinct from the

extrinsic effects of changed c_H , defect density or microstructure. These are the observed, although quantitatively unreliable, changes in c_H from infrared absorption measurements, and the observation of different photoluminescence changes (with x) when the preparatory method is changed. It therefore appears that both in this work and in earlier reported work in the literature,⁴ separation of intrinsic from extrinsic effects should be regarded as a major element of analysis.

Two comments relevant to devices may be made. First, we have noted that our earlier publication reporting a high preference ratio of Si—H to Ge—H bonds in these alloys must not be taken to imply a very large density of uncompensated defects on the Ge atoms, since the photoconductivity and photoluminescence of the alloys are much better than would be expected from the preference ratio data. We infer that in these hydrogenated alloys the preferred attachment of H to Si over Ge may even be the *result* of a reduced defect density on the Ge rather than the *cause* of an increased such density. Second, we conclude that despite differences in the detailed changes in the density of states in samples prepared by different methods, it appears that a general result is an overall increase in the extrinsic state density, especially in the lower half of the pseudogap, which leads to a decrease in the photoelectronic response. In particular, a decrease in both $(\mu\tau)_n$ and $(\mu\tau)_p$ is suggested. It has been proposed that $a\text{-Si}_{1-x}\text{Ge}_x\text{:H}$ may be useful as an intrinsic layer in amorphous thin-film solar cells, due to a better match of the optical gap to the solar radiation spectrum. The decrease in $(\mu\tau)_n$ and $(\mu\tau)_p$ proposed here, however, may offset the gain in device efficiency that could be achieved.

ACKNOWLEDGMENTS

We thank David MacLeod for the construction of the sample preparation system and for expert technical assistance. We also thank Paul Kirby, Djalil Lachter, Suha Oguz, Richard Weisfield, and Ben Yacobi for subsidiary characterizational measurements and helpful discussions. This work was supported by the U.S. Department of Energy under Contract No. DE-AC03-79-ET23036 and the Solar Energy Research Institute under Subcontract No. XW-1-9358-1.

- *Present address: Comsat Laboratories, 22300 Comsat Drive, Clarksburg, MD 20734.
- †Present address: Solar Power Corp., 20 Cabot Road, Woburn, MA 01801.
- ‡Present address: SERA Solar, 3151 Jay Street, Santa Clara, CA 95050.
- ¹D. K. Paul, B. von Roedern, S. Oguz, J. Blake, and W. Paul, *J. Phys. Soc. Jpn.* **49**, Suppl. A, 1261 (1980).
- ²W. Paul, in *Fundamental Physics of Amorphous Semiconductors*, Vol. 25 of *Springer Series in Solid State Sciences*, edited by F. Yonezawa (Springer, Heidelberg, 1981), p. 72.
- ³W. Paul, D. K. Paul, B. von Roedern, J. Blake, and S. Oguz, *Phys. Rev. Lett.* **46**, 1016 (1981).
- ⁴D. Hauschildt, R. Fischer, and W. Fuhs, *Phys. Status Solidi B* **102**, 563 (1980).
- ⁵M. H. Brodsky, *Thin Solid Films* **40**, L123 (1977).
- ⁶B. G. Yacobi, R. W. Collins, G. Moddel, P. Viktorovitch, and W. Paul, *Phys. Rev. B* **24**, 5907 (1981).
- ⁷S. Oguz, R. W. Collins, M. A. Paesler, and W. Paul, *J. Non-Cryst. Solids* **35-36**, 231 (1980).
- ⁸B. G. Yacobi (private communication).
- ⁹A. Onton, H. Wieder, J. Chevallier, and C. R. Guarnieri, in *Proceedings of the 7th International Conference on Amorphous and Liquid Semiconductors*, edited by W. E. Spear (CICL, University of Edinburgh, 1977), p. 357.
- ¹⁰G. Moddel, D. A. Anderson, and W. Paul, *Phys. Rev. B* **22**, 1918 (1980).
- ¹¹R. W. Collins, M. A. Paesler, and W. Paul, *Solid State Commun.* **34**, 833 (1980).
- ¹²R. A. Street, *Phys. Rev. B* **23**, 861 (1981); W. Paul and D. A. Anderson, *Solar Energy Mater.* **5**, 229 (1981).
- ¹³B. von Roedern and G. Moddel, *Solid State Commun.* **35**, 467 (1980).
- ¹⁴P. Viktorovitch and G. Moddel, *J. Appl. Phys.* **51**, 4847 (1980).
- ¹⁵G. Moddel, Thesis, Harvard University, Cambridge, Mass., 1981 (unpublished).
- ¹⁶G. S. Higashi and M. Kastner, *J. Phys. C* **12**, L821 (1979); see also C. M. Gee and M. Kastner, *Phys. Rev. Lett.* **42**, 1765 (1979); R. W. Collins and W. Paul, *Phys. Rev. B* **25**, 5257 (1982).
- ¹⁷G. Moddel, J. Blake, R. W. Collins, P. Viktorovitch, D. K. Paul, B. von Roedern, and W. Paul, in *Tetrahedrally Bonded Amorphous Semiconductors—1981, Carefree, Arizona*, edited by R. A. Street, D. K. Biegelsen, and J. C. Knights (American Institute of Physics, New York, 1981), p. 171.
- ¹⁸P. Viktorovitch, G. Moddel, J. Blake, S. Oguz, and William Paul, *J. Phys. (Paris)* **42**, 455 (1981).
- ¹⁹D. A. Anderson and W. E. Spear, *Philos. Mag. B* **36**, 695 (1977).
- ²⁰It is notable that in these alloys the preference ratio of Si—H to Ge—H bonds is at least as large as in our pure glow-discharge alloys.
- ²¹A. Morimoto, T. Miura, M. Kumeda, and T. Shimizu, *Jpn. J. Appl. Phys.* **20**, L833 (1981).
- ²²M. Cretella (private communication).